Reionized bubbles around primordial galaxies: exercises

Joris Witstok (joris.witstok@nbi.ku.dk)

February 26, 2025

1 Background problems: recombination lines in astrophysical nebulae

Given atomic number Z, the energy levels E_n in the classical Bohr (1913) model of an atom are

$$E_n \approx \frac{-13.6Z^2}{n^2}\,\mathrm{eV}\,. \tag{1}$$

Electronic transitions between energy levels $n \longrightarrow m$ then offer a natural theoretical explanation for the empirical Rydberg formula,

$$\frac{1}{\lambda} = RZ^2\left(\frac{1}{m^2} - \frac{1}{n^2}\right), \tag{2}$$

which relates spectral line wavelengths λ to a pattern based on a set of two integers, n and m ($n > m$).

Problem 1.1. Given the photon energy $E = hc/\lambda$, work out $R_\mathrm{H} \equiv R$, the Rydberg constant for hydrogen ($Z = 1$).

Problem 1.2.

(a) Using this atomic model of hydrogen, calculate the wavelengths of the principal spectral lines in the Lyman, Balmer, and Paschen series (Lyα, Hα, and Paα), corresponding to the $n + 1 \longrightarrow n$ electronic transitions for $n \in \{1, 2, 3\}$.

(b) Across what redshift range can we observe each of these lines with the low-resolution PRISM disperser of the JWST/NIRSpec[1] instrument? And with the medium-resolution G235M grating?

(c) How do the wavelengths of these spectral lines compare to the equivalent He II (singly ionised helium) electronic transitions?

Problem 1.3. Keeping in mind that electrons usually carry some kinetic energy, what is the energy of a photon produced in the event where hydrogen recombination ($H^+ + e^- \longrightarrow H^0$) directly results in the ground state ($n = 1$)? Explain why for case-B recombination we can make the so-called 'on-the-spot approximation', where only recombinations leaving hydrogen in one of the excited states ($n > 1$) are taken into account.

Problem 1.4. When evolving on the main sequence, spectral O-type stars may have a size ten times that of the Sun, effective surface temperature of 40 000 K, and emit hydrogen-ionising photons at a rate of $\dot{N}_\mathrm{ion} = 10^{49}\,\mathrm{s}^{-1}$. Consider a surrounding H II region consisting of pure hydrogen, with a number density of $n_\mathrm{H} = 300\,\mathrm{cm}^{-3}$.

(a) If the H II region is 4 parsec in diameter, would it be ionisation bounded? Check in the range of electron temperatures $10\,000\,\mathrm{K} < T_e < 30\,000\,\mathrm{K}$, where you can assume the (case-B) recombination rate of the gas to follow $\alpha_\mathrm{rec} = 2.54 \times 10^{-13}\,(T_e/10^4)^{-0.8}\,\mathrm{cm}^3\,\mathrm{s}^{-1}$.

(b) If roughly two out of three of recombination events lead to the emission of a Lyα photon (in the ionisation-bounded case), what is the Lyα luminosity of the cloud? How does this compare to the bolometric luminosity of the central star, if assumed to be a perfect blackbody?

[1] The wavelength coverage of the various NIRSpec instrument modes is documented here: https://jwst-docs.stsci.edu/jwst-near-infrared-spectrograph/nirspec-instrumentation/nirspec-dispersers-and-filters.

2 Background problems: measuring distances in an expanding universe

Problem 2.1. Assume the time evolution of an ionised bubble radius, $R_{\rm ion}(t)$, follows the differential equation given by Cen & Haiman (2000):

$$\frac{{\rm d}R_{\rm ion}^3}{{\rm d}t} = 3H(z)R_{\rm ion}^3 + \frac{3f_{\rm esc,\,LyC}\,\dot{N}_{\rm ion}}{4\pi\bar{n}_{\rm H}} - C_{\rm HII}\bar{n}_{\rm H}\alpha_{\rm B}R_{\rm ion}^3\,. \tag{3}$$

(a) If we only consider the cosmic expansion represented by the first term on the right-hand side, solve for $R_{\rm ion}(t)$. Work out the e-folding time at redshift $z = 7$ assuming a Planck Collaboration et al. (2020) cosmology, where the Hubble parameter is $H(z = 7) \approx 856.6\,{\rm km\,s^{-1}\,Mpc^{-1}}$. Is this effect important at this redshift? (Hint: compare to the age of the Universe at this redshift.)

(b) If we instead neglected the cosmic expansion and recombinations, how would $R_{\rm ion}(t)$ evolve in terms of the ionising photon production rate $N_{\rm ion}$ and escape fraction $f_{\rm esc,\,LyC}$ of the central galaxy? (Hint: see Mason & Gronke (2020) or Witstok et al. (2024).)

(c) Given the present-day ($z = 0$) cosmic mean hydrogen number density of $\bar{n}_{\rm H} \approx 1.88 \times 10^{-7}\,{\rm cm^{-3}}$, how large does an ionised bubble need to be for recombination events to balance the ionising output of a $z = 7$ galaxy, if it produces ionising photons at a rate of $N_{\rm ion} = 10^{54}\,{\rm s^{-1}}$, of which $f_{\rm esc,\,LyC} = 10\%$ escape? You can assume the IGM within the bubble to have mean density and recombination rate as in Problem 1.4(b) with $T_e = 20\,000\,{\rm K}$. What if the galaxy were at $z = 12$?

3 Application to the JADES spectroscopic galaxy survey

3.1 Summary of the exercise

In this exercise, we will use the method outlined in Witstok et al. (2024) to estimate the size of an ionised bubble. This will involve calculating the Lyα transmission curve for the two-zone model from Mason & Gronke (2020), where a photon trajectory starts inside a spherical ionised bubble (with a radius $R_{\rm ion}$) centred on the source, before travelling through the IGM characterised by a 'global' neutral fraction, $\bar{x}_{\rm H\,I}$. Then, given the intrinsic strength of Lyα predicted by converting the measured Hβ line luminosity, it is possible to work out a lower limit on $R_{\rm ion}$, the bubble radius.

3.2 Gather spectroscopic data and measure the redshift and line fluxes

We will be using NIRSpec spectra obtained as part of the JWST Advanced Deep Extragalactic Survey (JADES; Eisenstein et al. 2023) in the Great Observatories Origins Deep Survey (GOODS) extragalactic legacy fields located in the North (GOODS-N) and South (GOODS-S). Specifically, we will start by looking at source ID 1899 in a medium-depth tier of JADES covering the GOODS-N field, which was identified by Witstok et al. (2025) as one of the most distant known Lyα emitting galaxies (LAEs; see also Tang et al. 2024; Navarro-Carrera et al. 2024).

NIRSpec spectroscopy in JADES is taken in the PRISM disperser operating at low spectral resolution across 1-5 µm, as well as in the medium-resolution G140M, G235M, and G395M gratings (see Problem 1.2). Fully reduced and science-ready observations from JADES are publicly available on the Mikulski Archive for Space Telescopes (MAST). A dedicated MAST web page (`https://archive.stsci.edu/hlsp/jades`) describes how we can access the high-level science products (HLSP) via the PYTHON package ASTROQUERY.

(a) Run the relevant code block in the notebook to download the PRISM/CLEAR, G140M, and G395M spectra of ID 1899 onto your local machine.

(b) Open the preview of the PRISM spectrum. This shows the one-dimensional spectrum, which is extracted from the two-dimensional spectrum (how the dispersed light will show up on the detector). Why is the central trace with positive signal-to-noise ratio (SNR) surrounded by two negative traces on either side?

(c) Plot the one-dimensional spectra by reading in the downloaded `*x1d` files in FITS (Flexible Image Transport System) format.

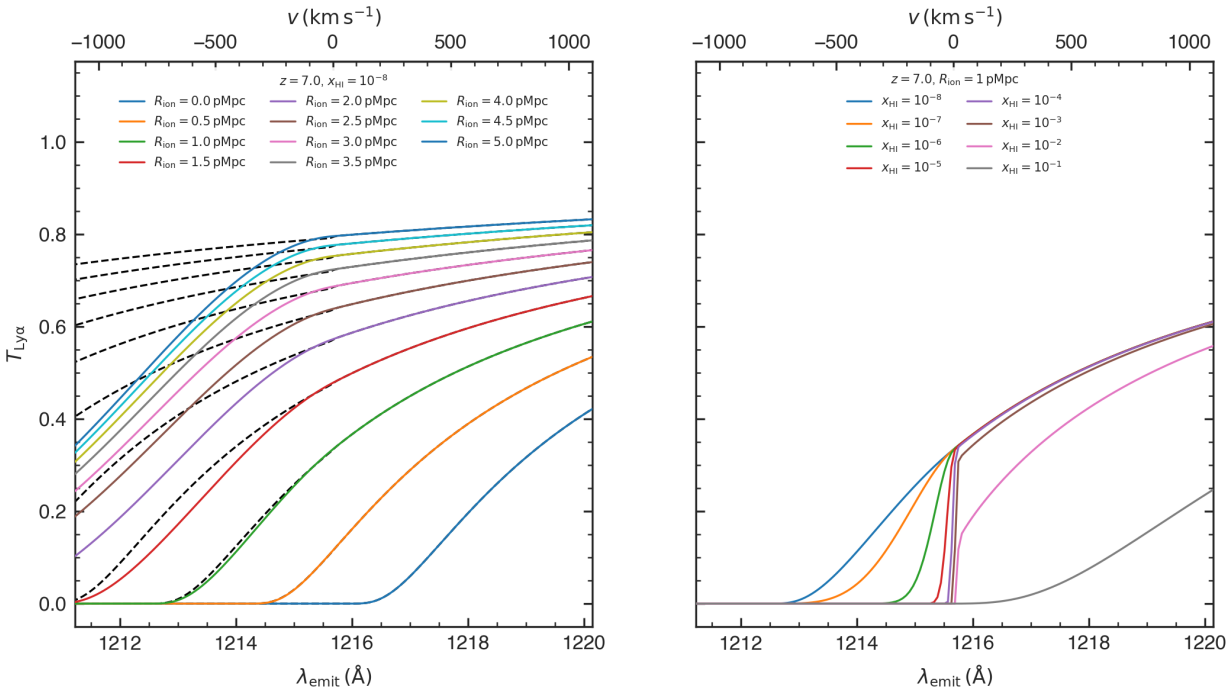

Figure 1: IGM transmission curves, reproduced as Figure 1 from Mason & Gronke (2020).

Several strong rest-frame optical emission lines are observed at the red of the spectrum covered by the G395M grating, from which we can measure a redshift, $z = \lambda_{\rm obs}/\lambda_{\rm emit} - 1$. At sufficiently high redshift (as is the case for ID 1899), the strong Hα line shifts out of the NIRSpec wavelength range. However, there is still the Hβ at a rest-frame wavelength of 4862.71 Å, as well as two strong emission lines of [O III] are located at 4960.295 Å and 5008.24 Å. The luminosity ratio between the [O III] lines is determined by atomic physics to be $F_{5008}/F_{4960} \approx 2.98$ across a range of temperatures and densities applicable to H II regions (where the majority of the [O III] emission is produced).

(d) What is the highest redshift Hα can be seen with NIRSpec? And Hβ?

(e) Given its spectral resolution of at least $R \approx 1000$ in the observed G395M spectrum, what is the expected precision (its standard deviation σ_z) of our redshift measurement? Assume the line spread function (LSF) is Gaussian, with full-width at half maximum (FWHM) $\Delta\lambda$ relating to R via $R \equiv \lambda/\Delta\lambda$. (Hint: you can convert the FWHM of a Gaussian to the standard deviation σ by dividing by a factor $2\sqrt{2\ln(2)} \approx 2.35$.)

(f) Construct a model of Gaussian line profiles to measure the redshift from the Hβ and [O III] lines observed at 4.4-4.9 μm in the G395M spectrum. You can assume the spectral resolution to be constant value of $R = 1500$ across this wavelength range, and an intrinsic line width ranging across $0 < \sigma_{\rm int} < 500\,{\rm km\,s^{-1}}$. Does the uncertainty on the redshift measurement match your estimate from above (if not, why)?

(g) With the measured systemic redshift, fit a Gaussian profile to the Lyα line in the G140M spectrum (NB: the line centre may be resonantly scattered away from the systemic redshift; see Appendix A.3 for the relevant conversions). From the luminosity ratio between Lyα and Hβ, determine the escape fraction of Lyα, $f_{\rm esc,\,Ly\alpha}$.

Now we will repeat the exercise for (much fainter) source ID 10013682 in the DEEP/HST tier of JADES, which was first identified as a remarkably strong LAE in the GOODS-S field by Saxena et al. (2023).

(h) Given the lower SNR in the G395M spectrum, perform your redshift measurement on the lower-resolution PRISM data this time ($R \approx 100$; how is the precision expected to change?). For the fit, you can assume $R = 350$ at $\lambda_{\rm obs} > 4$ μm.

(i) With the measured systemic redshift, again measure the strength of the Lyα line in the G140M spectrum and estimate $f_{\rm esc,\,Ly\alpha}$.

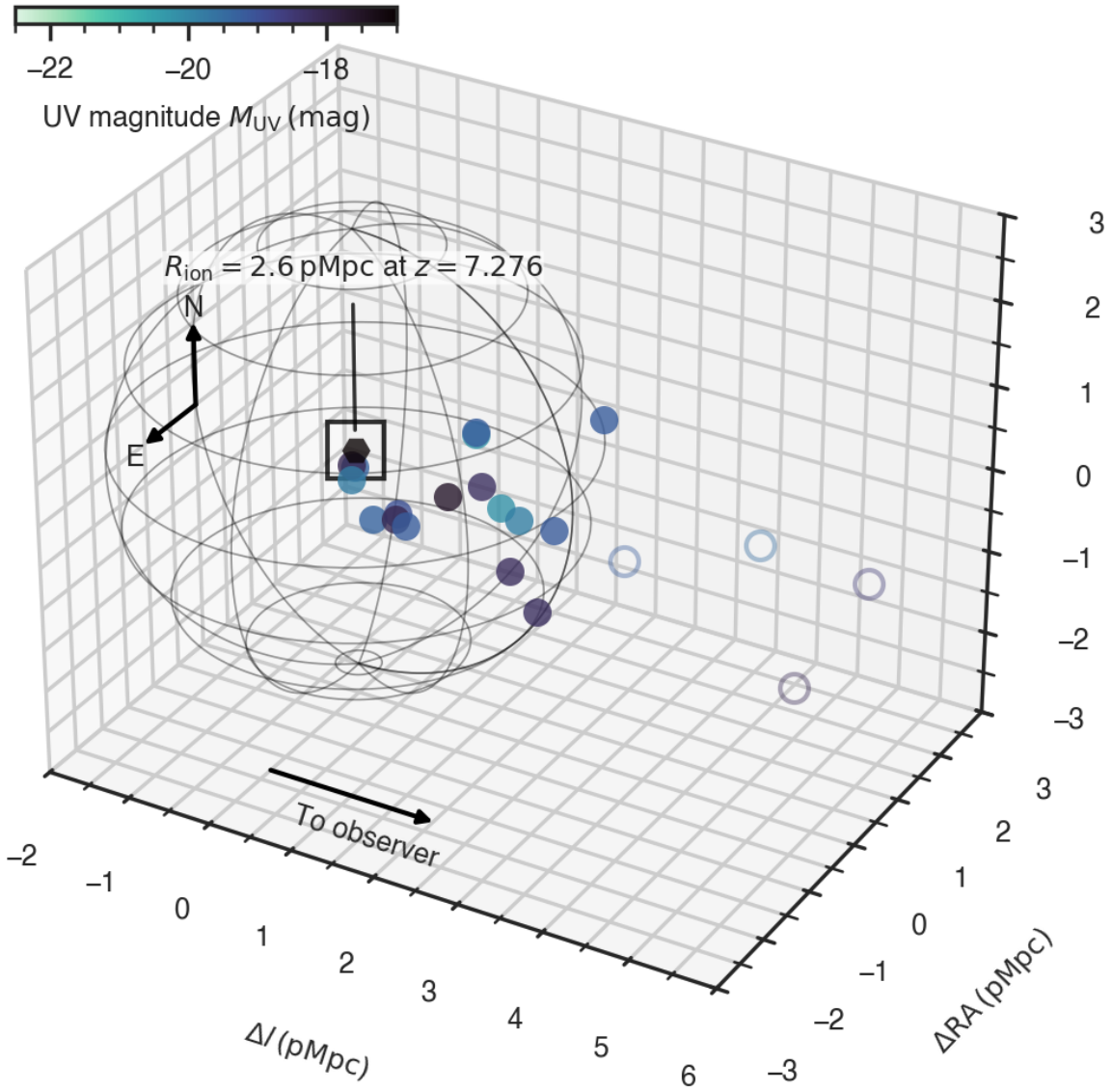

Figure 2: Neighbouring galaxies in the ionised bubble of ID 10013682 (partial reproduction of Figure 5 in Witstok et al. 2024).

3.3 Validate against literature

From here on, we will focus on source ID 10013682 to study the ionised bubble it resides in. Compile the relevant measurements from Witstok et al. (2024), where ID 10013682 was analysed among a sample of high-redshift LAEs in JADES. We will need its sky coordinates, spectroscopic redshift, UV magnitude, the Lyα velocity offset $\Delta v_{\mathrm{Ly}\alpha}$ and escape fraction, $f_{\mathrm{esc,\,Ly}\alpha}$, which are summarised in Table 1. How do your measurements from Section 3.2 compare to those reported in Witstok et al. (2024)?

3.4 Install prerequisites and calculate IGM transmission curves

Check whether you have installed the right modules by running the first code block. Download the PYTHON module LYMANA-ABSORPTION from `https://github.com/joriswitstok/lymana_absorption`. Verify that the code works by running the code block that reproduces Figure 1 from Mason & Gronke (2020), as shown in Fig. 2.

3.5 Calculate ionised bubble size

Finally, we will estimate the ionised bubble radius that ID 10013682 resides in. Following Witstok et al. (2024), we are looking for the value of R_{ion} at which the IGM transmission at the measured Lyα velocity offset is equal to the estimated Lyα escape fraction to find an effective lower limit on R_{ion}.

(a) Predict the IGM transmission at the measured Lyα velocity offset $\Delta v_{\mathrm{Ly}\alpha}$ for a range of ionised bubble sizes (logarithmically spaced between 1 pkpc and 10 pMpc), and estimate (through interpolation) at which ionised bubble radius R_{ion} the IGM transmission becomes equal to the Lyα escape fraction.

(b) Why does this effectively yield a lower limit on R_{ion}? What are the caveats of estimating R_{ion} with this method?

(c) Inexcusably, Witstok et al. (2024) do not report uncertainties on their inferred bubble radii. Just considering the uncertainty on $\Delta v_{\mathrm{Ly}\alpha}$, what range of R_{ion} do you find?

(d) Given its absolute UV magnitude[2] of $M_{\mathrm{UV}} \approx -17$ mag and ionising photon efficiency directly measured to be $\log \xi_{\mathrm{ion}} = 25.66\,\mathrm{Hz\,erg^{-1}}$ by Saxena et al. (2024), how long would it take ID 10013682 to create this ionised region itself if it had an escape fraction 100%? (Hint: use (i) Appendix A.2 to convert M_{UV} to a flux density $F_{\nu,\,\mathrm{UV}}$, (ii) Appendix A.1 to obtain the luminosity density $L_{\nu,\,\mathrm{UV}}$, (iii) the fact that $\dot{N}_{\mathrm{ion}} = \xi_{\mathrm{ion}} L_{\nu,\,\mathrm{UV}}$, and (iv) your solution from Problem 2.1(b) to calculate the required age.)

3.6 Visualise the environment of the ionised bubble

The NIRCam wide-field slitless spectroscopic mode allows an efficient way to obtain spectra of a large number of galaxies. This has been exploited in the FRESCO survey (Oesch et al. 2023) covering both the GOODS fields, allowing a 'blind' redshift search up to $z \approx 8$.

(a) Using the catalogue provided by Helton et al. (2024), plot all nearby galaxies in the GOODS-S field that have been spectroscopically confirmed close to ID 10013682 (within approximately 5 pMpc).

(b) Assuming the relations from Mason & Gronke (2020) to link the absolute UV magnitude M_{UV} and UV slope β_{UV} of a galaxy to its ionising photon production rate,

$$\dot{N}_{\mathrm{ion}} = 1.65 \times 10^{54}\, 10^{\frac{M_{\mathrm{UV}}+20}{-2.5}} \left(\frac{912.0}{1500.0}\right)^{\beta_{\mathrm{UV}}+2} \mathrm{s^{-1}},$$

by how much do galaxies contained within the bubble increase the available ionising-photon budget from Section 3.5(c)? Does this alleviate the tension with the inferred size required to explain the Lyα emission?

[2] See `https://en.wikipedia.org/wiki/Absolute_magnitude`.

References

Bohr N., 1913, Philosophical Magazine, 26, 1

Cen R., Haiman Z., 2000, ApJ, 542, L75

Eisenstein D. J., et al., 2023, p. arXiv:2306.02465 (arXiv:2306.02465)

Helton J. M., et al., 2024, ApJ, 974, 41

Mason C. A., Gronke M., 2020, MNRAS, 499, 1395

Navarro-Carrera R., Caputi K. I., Iani E., Rinaldi P., Kokorev V., Kerutt J., 2024, p. arXiv:2407.14201 (arXiv:2407.14201)

Oesch P. A., et al., 2023, MNRAS, 525, 2864

Oke J. B., Gunn J. E., 1983, ApJ, 266, 713

Planck Collaboration et al., 2020, A&A, 641, A6

Saxena A., et al., 2023, A&A, 678, A68

Saxena A., et al., 2024, A&A, 684, A84

Tang M., Stark D. P., Topping M. W., Mason C., Ellis R. S., 2024, ApJ, 975, 208

Witstok J., et al., 2024, A&A, 682, A40

Witstok J., et al., 2025, MNRAS, 536, 27

A Lookup

A.1 Converting between flux and flux densities F_ν and F_λ

$$
\begin{aligned}
F &= \frac{L}{4\pi d^2} \\
F_\nu &= \frac{F}{\Delta\nu}, \quad F_\lambda = \frac{F}{\Delta\lambda} \\
\lambda &= \frac{c}{\nu} \\
\frac{\mathrm{d}\lambda}{\mathrm{d}\nu} &= -\frac{c}{\nu^2} \\
\mathrm{d}\nu F_\nu &= \mathrm{d}\lambda F_\lambda \\
F_\nu &= \left|\frac{\mathrm{d}\lambda}{\mathrm{d}\nu}\right| F_\lambda = \frac{c}{\nu^2} F_\lambda = \frac{\lambda^2}{c} F_\lambda
\end{aligned}
$$

A.2 Magnitude system

With AB magnitude m_{AB} as defined by (Oke & Gunn 1983):

$$
\begin{aligned}
m_1 - m_2 &= -2.5 \log_{10}\left(F_1/F_2\right) \\
m_{\mathrm{AB}} &= -2.5 \log_{10}\left[F_\nu \left(\mathrm{erg\,s^{-1}\,cm^{-2}\,Hz^{-1}}\right)\right] - 48.60 \\
&= 31.4 - 2.5 \log_{10}\left[F_\nu \left(\mathrm{nJy}\right)\right]
\end{aligned}
$$

A.3 Convenient conversions in frequency/wavelength/velocity space

$$\lambda = \frac{\lambda_{\rm line}}{1-\frac{\Delta v}{c}}, \quad \nu = \nu_{\rm line}\left(1-\frac{\Delta v}{c}\right)$$

$$\Delta\lambda = \lambda - \lambda_{\rm line} = \frac{\lambda_{\rm line}}{\frac{c}{\Delta v}-1}, \quad \Delta\nu = \nu - \nu_{\rm line} = -\frac{\Delta v}{c}\nu_{\rm line}$$

$$\Delta v = \left(1-\frac{\lambda_{\rm line}}{\lambda}\right)c = \frac{c}{1+\frac{\lambda_{\rm line}}{\Delta\lambda}} = -\frac{\Delta\nu}{\nu_{\rm line}}c$$

$$= \frac{c}{1+R} = \frac{zc}{1+z} \approx zc \ (z \ll 1)$$